

VU Research Portal

Kinematic analysis of the drag flick in field hockey

Ibrahim, R.; Faber, G.S.; Kingma, I.; van Dieen, J.H.

published in

Sports Biomechanics
2017

DOI (link to publisher)

[10.1080/14763141.2016.1182207](https://doi.org/10.1080/14763141.2016.1182207)

[Link to publication in VU Research Portal](#)

citation for published version (APA)

Ibrahim, R., Faber, G. S., Kingma, I., & van Dieen, J. H. (2017). Kinematic analysis of the drag flick in field hockey. *Sports Biomechanics*, 16(1), 45-57. <https://doi.org/10.1080/14763141.2016.1182207>

General rights

Copyright and moral rights for the publications made accessible in the public portal are retained by the authors and/or other copyright owners and it is a condition of accessing publications that users recognise and abide by the legal requirements associated with these rights.

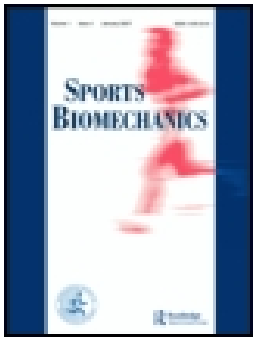
- Users may download and print one copy of any publication from the public portal for the purpose of private study or research.
- You may not further distribute the material or use it for any profit-making activity or commercial gain
- You may freely distribute the URL identifying the publication in the public portal ?

Take down policy

If you believe that this document breaches copyright please contact us providing details, and we will remove access to the work immediately and investigate your claim.

E-mail address:

vuresearchportal.ub@vu.nl



Kinematic analysis of the drag flick in field hockey

Rony Ibrahim, Gert S. Faber, Idsart Kingma & Jaap H. van Dieën

To cite this article: Rony Ibrahim, Gert S. Faber, Idsart Kingma & Jaap H. van Dieën (2016): Kinematic analysis of the drag flick in field hockey, Sports Biomechanics

To link to this article: <http://dx.doi.org/10.1080/14763141.2016.1182207>



Published online: 18 May 2016.



Submit your article to this journal [↗](#)



View related articles [↗](#)



View Crossmark data [↗](#)

Kinematic analysis of the drag flick in field hockey

Rony Ibrahim, Gert S. Faber, Idsart Kingma and Jaap H. van Dieën

Faculty of Behavioural and Movement Sciences, Department of Human Movement Sciences, Vrije Universiteit, Amsterdam, The Netherlands

ABSTRACT

Attaining high speed of the stick head and consequently of the ball is essential for successful performance of the drag flick in field hockey, but the coordination pattern used to maximise stick head speed is unknown. The kinematics of the drag flick was studied in ten elite hockey players who performed twenty shots each towards a target located 1.5 m high. A 150 Hz active marker motion analysis system was used, alongside two force plates to detect foot touchdown. Angular velocity and contribution to stick endpoint speed of upper body joints were analysed. Repeated measures ANOVA was used to compare timing of onset and peak angular velocities between joints. Participants used a kinematic pattern that was close to a proximal-to-distal sequence. Trunk axial rotation and lateral rotation towards the target, right wrist flexion and left wrist extension were the main contributors to stick endpoint speed. Coaches should emphasise trunk rotations and wrist flexion and extension movements for maximising stick head speed. Given the high level of the participants in this study, the coordination of joints motions, as reported here, can serve as a guideline for drag flick training.

ARTICLE HISTORY

Received 13 September 2015
Accepted 20 April 2016

KEYWORDS

Proximal-to-distal; stick; 3D kinematics; strength and conditioning; kinetic chain

1. Introduction

When aiming to improve athletic performance, a thorough analysis of skilled performance assessing the functionality of its characteristics is fundamental. Several researchers have studied explosive throwing, hitting and kicking skills in this way and found that highly skilled athletes usually accelerate the end effector (i.e. hand, foot, stick, club, etc.) by initiating the movement with the heaviest, proximal segment (i.e. trunk) followed by a proximal-to-distal sequence (Elliott, Marshall, & Noffal, 1995; Kellis & Katis, 2007; Liu, Leigh, & Yu, 2010; Marshall & Elliott, 2000; Reeser, Fleisig, Bolt, & Ruan, 2010; Wagner, Pfustershmed, Von Duvillard, & Müller, 2011). This has been described as the 'kinetic link principle', which states that kinetic energy of a segment is transferred to the adjacent, distal segment, as soon as it reaches its maximum, such that each segment starts or accelerates its motion relative to the proximal segment, when the adjacent proximal segment reaches its peak velocity (Marshall & Elliott, 2000; Putnam, 1993). In contrast to the observed strategy, the 'principle of optimal coordination of partial momenta' (Hochmuth, 1974; Putnam,

1993) predicts based on mechanical considerations that the speed of the end effector would only be maximised, if all the relevant joints would simultaneously reach their peak angular velocities and be fully extended to have the longest moment arm relative to the end effector. However, anatomical and physiological constraints make the kinetic link principle the more commonly adopted and most likely optimal strategy (Bobbert, Gerritsen, Litjens, & Van Soest, 1996; Elliott et al., 1995; Liu et al., 2010; Putnam, 1993; Reeser et al., 2010; Wagner et al., 2011).

The drag flick is an effective shooting technique in field hockey, especially when it comes to the penalty corner (McLaughlin, 1997; Piñeiro, Sampedre, & Refoye, 2007; Yusoff, Hasan, & Wilson, 2008). As opposed to hitting the ball, the drag flicker is allowed to elevate the ball at goals, thus making it a much more threatening alternative to hitting from the penalty corner as direct hitting shots on goals are not allowed to be above backboard height (46 cm). The drag flick is a multi-joint coordination task that involves both upper limbs in a closed chain. The rules of field hockey constrain the athlete to drag the ball along with the stick head and then flick it, instead of just hitting it as in other closed-chain shooting tasks (e.g. baseball batting, golf swinging). However, as in other single and double limb throwing and hitting tasks, the aim of the drag flick shot is to shoot the ball as accurate and as fast as possible.

Previous studies identified a wide stance and a whipping action of the stick followed by explosive sequential rotations of the pelvis, upper trunk and stick as determinants of a successful drag flick (López de Subijana, Juarez, Mallo, & Navarro, 2010; McLaughlin, 1997). However, the information provided by these studies was limited by either limitations in instrumentation, in particular a limited sample rate, or the skill level of the participants. Furthermore, both studies only analysed the kinematics of the pelvis, thorax and stick and neglected the kinematics of the upper limbs. Therefore, the goal of this study was to conduct a comprehensive 3D kinematic analysis of the drag flick in elite athletes.

Based on the preference for a proximal-to-distal sequence in throwing and hitting motions reported previously, it could be hypothesised that hockey players follow the kinetic link principle and adopt a proximal-to-distal sequence in the drag flick. However, unlike previously studied sports movements, the drag flick is performed with two arms in a closed loop and with extended contact between the implement and ball; hence, conventional proximal-to-distal sequencing might not be fully satisfied. Furthermore, we hypothesised that the trunk segment and all upper limbs joints contribute substantially to the endpoint speed.

2. Methods

Ten male field hockey players, mean (standard deviation) age 25 (3) years, mass 83 (5) kg and height 183 (3) cm, participated in this study. The participants were the following: three Olympic-level drag flickers, four national-level drag flickers and three Olympic-level hockey players (not specialised in drag flick). Before performing the experiment, participants signed informed consent. For each participant, anthropometric data, age and injury history were gathered. The participants did not suffer from an injury that prevented them from performing the drag flick at their maximal power or caused them to adapt a different movement pattern. The Ethics Committee of the Faculty of Human Movement Sciences of the VU University Amsterdam had approved the research protocol.

2.1. Data collection and pre-processing

Before starting the measurements, the athletes performed a warm-up routine, which included a number of progressively faster drag flicks. Each participant was then instructed to perform, using his own stick, twenty drag flicks with the ball positioned 13 m centrally in front of a target, which was at a height of 1.5 m. This target height is considered to be the most common for drag flicks in game situation, given the fact that players are allowed to perform low shots, below backboard height (46 cm), by hitting the ball instead of pushing it.

An active marker motion analysis system (Optotrak 3020, Northern Digital Inc., Ontario, Canada) was used after calibration with a cube with 16 markers. The system consisted of four arrays, containing three cameras each. It was used to capture, at 150 Hz, 3D coordinates data of twenty-seven markers. Eight cluster markers were strapped on different body segments (shanks, pelvis, thorax, upper arms and forearms), and the thighs were modelled between the shanks and pelvis, in order to obtain a full body model. In addition, three single markers were attached to the stick (1 marker on the shaft and 2 on the stick head). Anatomical coordinate systems of the segments were related to the corresponding marker clusters by digitising specified anatomical landmarks (Appendix 1) using a probe with six markers (Cappozzo, Catani, Della Croce, & Leardini, 1995). In the same way, the edges and endpoint of the stick were related to the markers on the stick. A dynamic 3-D linked segment model was used, wherein shoulder joint centre position was estimated based on the work of De Leva (1996) and shoulder rotation was the motion of the upper arm with respect to the trunk. Details of the original model and the modifications for more accurate anatomical modelling of the body segments can be found elsewhere (Faber, Chang, Kingma, & Dennerlein, 2013; Faber, Kingma, & van Dieën, 2011; Kingma, de Looze, Toussaint, Klijnsma, & Bruijnen, 1996).

Two custom-made strain gauge-based, 1×1 m, force plates (Vrije Universiteit, Amsterdam, The Netherlands) were used in order to measure the timing of right and left foot touchdown. Force plates and drag area were covered by artificial hockey grass (Figure 1).

Two high-speed cameras were used to visualise the motion. The first camera was placed on the right side to capture, at 240 Hz, the motion in the sagittal plane and was not used for data analysis (Casio EX-ZR1000, Casio Computer CO., LTD., Tokyo, Japan). The second camera was placed above the drag area to capture, at 140 Hz, the motion in the transverse plane and it was also used to detect ball release and calculate ball speed

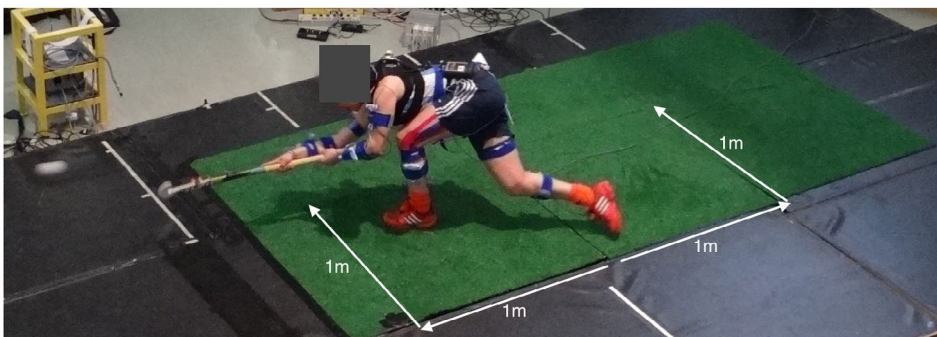


Figure 1. Photograph of the drag flick shot that was performed during the experiment. The two forceplates (1×1 m), which were covered by Astroturf, are highlighted.

(Basler avA1000-100gc, Basler AG, Ahrensburg, Germany). A LED light turned on when the Optotrak system started recording and was used to synchronise Optotrak with the top camera. The top camera provided projected ball speed instead of actual speed. However, the projection error is rather small and constant between trials, and this does not affect the result of this study because ball speed was only used as a selection criterion.

Due to the fact that the drag flick is an explosive movement with a large range of motion, gaps in the kinematic data occurred occasionally when markers were out of sight. These gaps were interpolated using a cubic spline function, for a maximum gap length of three samples. Subsequently, a bidirectional second-order low-pass Butterworth filter with a cut-off frequency of 15 Hz was used, to smooth the data.

2.2. Data analysis

2.2.1. Detection of ball release

Agreement between ball release detected from the video analysis (top camera) and from peak stick linear velocity in the direction of the target (Jennings et al., 2010) was assessed using the root-mean-square difference (RMSD). We found an average RMSD over participants of 3.4 ms, which supports the validity of both methods. In this paper, ball release was based on the latter method.

2.2.2. 3D kinematics

All kinematic analysis was carried out using custom software in MATLAB (R2012b, MathWorks inc. US). The angular velocity of the trunk segment (ω_T) was calculated with respect to the global coordinate system (Berme & Capozzo, 1990). The angular velocities in shoulders, elbows and wrists were calculated by first expressing the velocity of the distal segment relative to the proximal one and then using the equation of Berme and Capozzo (1990). Given the difficulty of measuring the 3D kinematics of the hand, we assumed that the hands and stick rotated together as a rigid unit. The wrist angular velocity was calculated as the angular velocity of the stick with respect to the forearm. The drag flick is initiated by a sidestep jump, followed by right foot touchdown, ball pickup, left foot touchdown, drag phase, flick phase and follow-through. The drag phase starts at left foot touchdown, and it occupies the largest percentage of shot time and serves to accelerate the ball up to a high speed after which the ball is further accelerated in the subsequent flick phase. Based on the opinion of coaches and players, the start of the flick phase is indicated by the onset of right wrist flexion, and during this phase, the actual shooting motions take place. Only angular velocity components that reached a substantial peak angular velocity during the flick phase, i.e. on average higher than 300 deg/s, were selected for analysis of the adopted kinematic pattern.

2.2.3. Contribution of joints motions to stick endpoint velocity

By modelling the hockey player, separately for each arm, as a chain with the L5S1 joint as the proximal point and the stick head S as the distal endpoint, and assuming that all body segments in the chain are rigid, the linear velocity of stick head (V_S) can be regarded as the sum of the linear velocities contributed by the absolute linear velocity of the L5S1 joint (V_{L5S1}), the angular velocity of the trunk segment relative to the global coordinate system (ω_T), and the angular velocities at the shoulder, elbow and wrist joints of one upper limb:

$$V_S = V_{L5S1} + \omega_T \times r_{L5S1,S} + \sum_{j=1}^q \omega_j \times r_{j_c,S}$$
 (1)

where the subscript *j* indicates the joint (shoulder, elbow and wrist of the right or left arm), ω_j is the 3D joint angular velocity expressed with respect to the global coordinate system. $r_{j_c,S}$ is the position vector from joint centre to the stick head (*S*), and $r_{L5S1,S}$ represents the position vector from L5S1 joint to *S*. For further clarification, the contribution of trunk rotations to stick head linear velocity is quantified by the term ' $\omega_T \times r_{L5S1,S}$ ', and the contribution of each joint *j* of the right or left upper limb to V_S is quantified by the term ' $\omega_j \times r_{j_c,S}$ '.

After averaging over participants, we compared the left to the right side of equation 1 for each upper limb over time. Our results showed high correlations between the time series with correlation coefficients of 0.99 and an average RMSE of 1.1 m/s for both upper limbs, thereby supporting the validity of our 3D model and method. The RMSE between both time series can be explained by errors in calculated joint centre positions, due to measurement errors (e.g. skin movement, muscle contraction under the cluster, interpolation), and the assumption of rigid segments and pure ball-and-socket joints (no joint translation).

2.3. Statistical analysis

Velocity time series were time normalised from left foot touchdown until ball release and represented as percentage of the normalised time (NT), with left foot touchdown 0% and ball release 100%. All data are presented as mean (standard deviation). The timing of the noted peak joints angular velocities (Table 1), of the best trial for each participant, defined as the trial with the highest ball speed, was compared between joints with one-way repeated measures ANOVA. If the results of one-way ANOVAs showed a significant main effect, then paired t-tests with Bonferroni correction were used to identify between which specific joints the timing of peak angular velocities differed significantly from the nearby peak in another joint. The same was done for the onset of these distinguished joints angular velocities. Two participants needed to be omitted from the analysis for the left arm due to marker visibility issues. All statistical analyses were carried out using IBM SPSS Statistics 20.

Table 1. All calculated joint angular velocities and their peak magnitudes during the drag flick.

Joint	Rotation around x-axis mean (SD) deg/s	Rotation around y-axis mean (SD) deg/s	Rotation around z-axis mean (SD) deg/s
Trunk	Lateral flexion left 614 (98) No lateral flexion right	Flexion 223 (92) Extension 136 (90)	Axial rotation left 579 (120) No axial rotation right
Right shoulder	Abduction 252 (218) Adduction 438 (137)	Flexion 779 (192) Extension 201 (99)	External rotation 132 (279) No internal rotation
Right elbow	No rotations	Flexion 267 (81) Extension 660 (230)	Pronation 293 (173) Supination 555 (192)
Right wrist	Radial deviation 169 (150) Ulnar deviation 114 (122)	Flexion 1,389 (286) Extension 709 (117)	No rotations
Left shoulder	Abduction 345 (193) Adduction 726 (335)	Flexion 585 (204) Extension 218 (208)	External rotation 542 (92) Internal rotation 435 (218)
Left elbow	No rotations	Flexion 247 (89) Extension 103 (165)	Pronation 22 (273) Supination 238 (263)
Left wrist	Radial deviation 553 (196) Ulnar deviation 230 (265)	Flexion 1,050 (205) Extension 976 (296)	No rotations

3. Results

3.1. Kinematic pattern

Our results showed that the drag phase lasted up to 81.5%, which is the moment when the flick phase started. The ball travelled a total distance of around 2.5 m from ball pickup to ball release and was released with a velocity of 31.7 (2.5) m/s towards the target. Selected joint angular velocity time traces are presented for the trunk and right arm in Figure 2 and for the trunk and left arm in Figure 3. During the drag phase, right elbow pronation and left shoulder external rotation velocity reached their peak values first. Subsequently, right wrist extension, left wrist flexion, right elbow supination and right shoulder adduction velocity reached their peak values between 60 and 70% of NT. The drag was then concluded with peaks in trunk axial rotation, left shoulder flexion and left shoulder adduction velocity.

For the relevant joint motions (shown in Figures 2 and 3), Figure 4 illustrates the peaks during the flick phase and Figure 5 shows the timing of their onset (i.e. a change of the sign). A significant effect of joint on normalised peak times ($p < 0.001$) was found. In line with the hypothesised proximo-distal sequence, pairwise comparisons (Figure 4) showed that the sequence of the torso and left upper limb peak joints angular velocities was (1) torso lateral rotation, left shoulder internal rotation, left wrist radial deviation and (2) left wrist extension ($p < 0.05$). The sequence for the right upper limb joint rotations peaks was (1) torso lateral rotation, (2) right shoulder flexion and (3) right wrist flexion and right elbow extension ($p < 0.05$). In addition, a significant effect of joint on normalised onset times ($p < 0.001$) was found. Pairwise comparisons (Figure 5) showed that the sequence of onset times of the torso and left upper limb joint rotations was (1) torso lateral rotation,

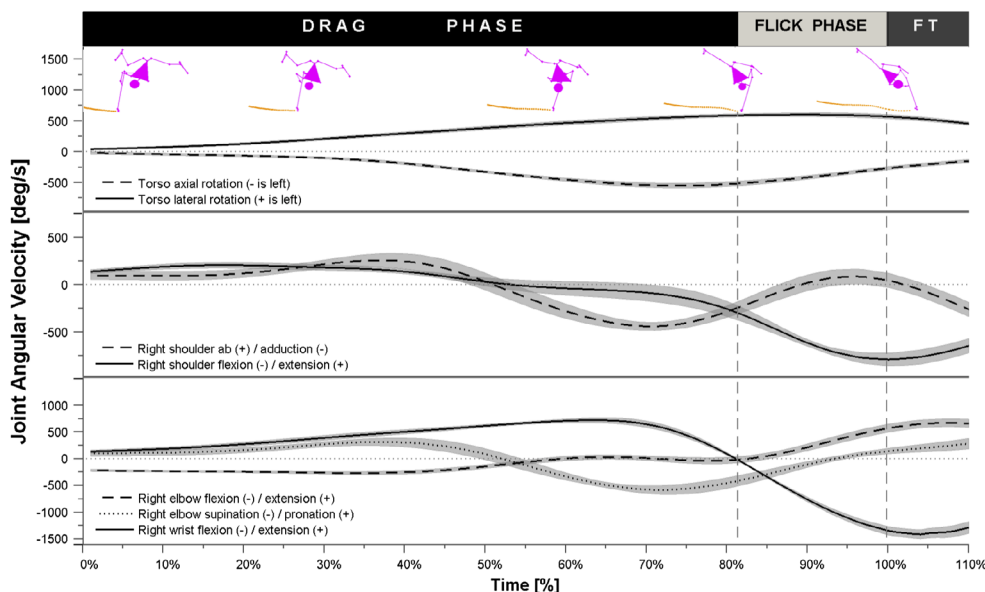


Figure 2. Trunk and right upper limb mean joint angular velocity, in black solid and dashed line (refer to the subfigure legend), normalised over time and averaged over participants' best trial, and the standard error in grey shading. At the top, 3 main phases are highlighted: the drag phase, flick phase and follow-through (FT). 5 captures of the 3D model (top-view) are inserted in correspondence to the NT and aim to improve the visualisation of the kinematic pattern.

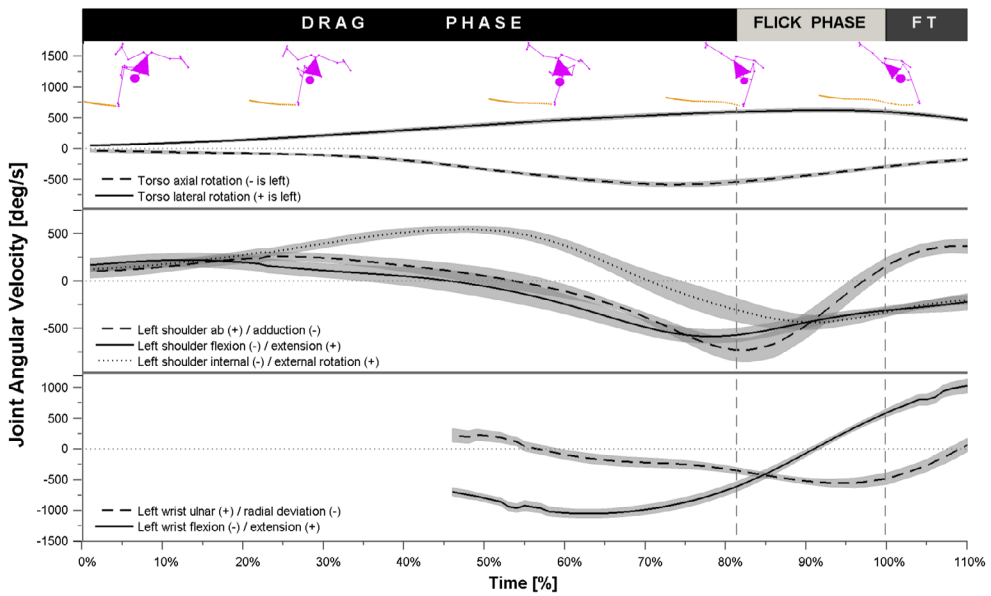


Figure 3. Trunk and left upper limb mean joint angular velocity in black solid and dashed line (refer to the subfigure legend), normalised over time and averaged over participants' best trial, and the standard error in grey shading. Refer to caption of Figure 2.

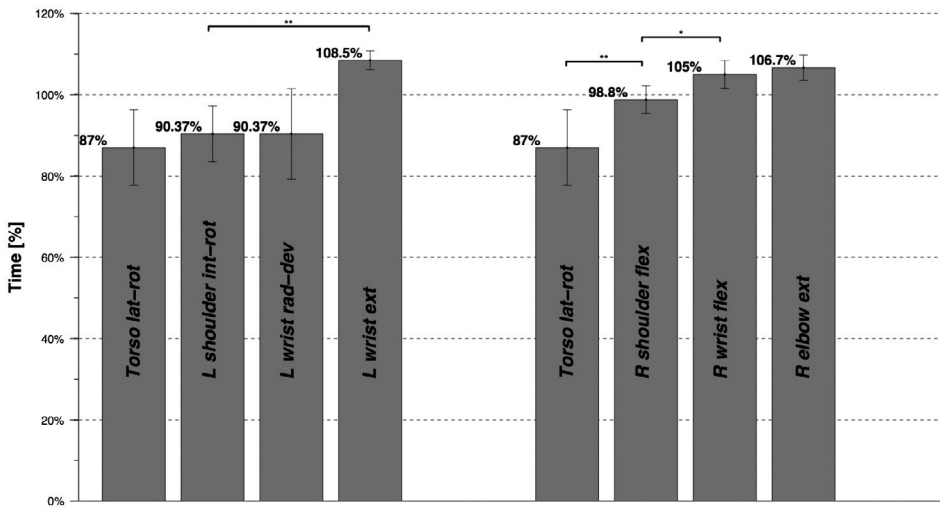


Figure 4. Timing of peak joints angular velocity during the flick phase (* $p < 0.05$ and ** $p < 0.01$). Left foot touchdown is 0% and ball release is 100%.

(2) left wrist radial deviation and left shoulder internal rotation and (3) left wrist extension ($p < 0.05$). The sequence for right upper limb joint rotations onset was (1) torso lateral rotation, (2) right shoulder flexion, right elbow extension and right wrist flexion ($p < 0.01$).

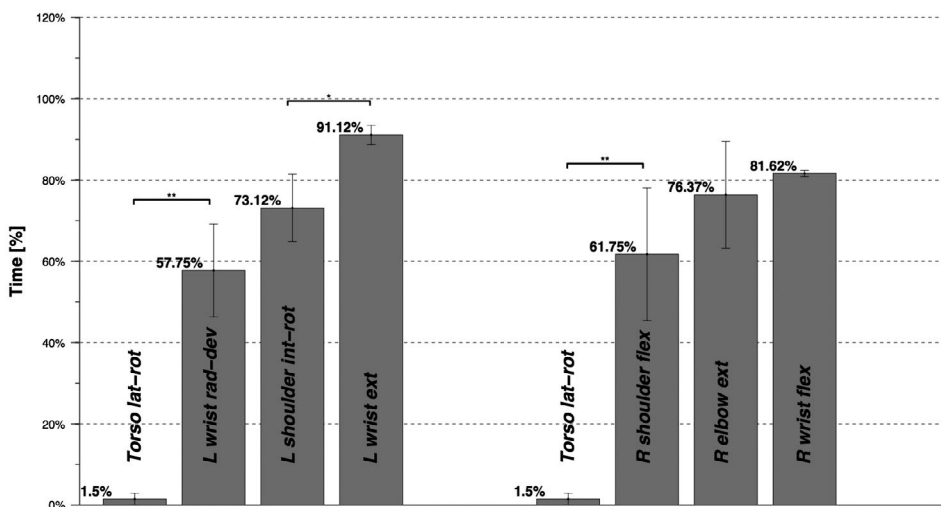


Figure 5. Timing of onset joints angular velocity that had their peaks during the flick phase (* $p < 0.05$ and ** $p < 0.01$). Left foot touchdown is 0% and ball release is 100%.

3.2. Contributions to stick endpoint velocity

During the drag phase, peak negative contributions of the right and left wrist (Figures 6 and 7) coincided with peak right wrist extension and left wrist flexion (Figures 2 and 3), corresponding to a phase lag of the stick relative to the right forearm. The right shoulder showed a peak positive contribution during the last part of the drag phase (Figure 6), caused by right shoulder peak adduction (Figure 2), bringing the upper arm in line with the trunk.

At the end of the drag and start of the flick phase, the left shoulder showed a peak positive contribution, mainly caused by peak left shoulder adduction and internal rotation (Figure 3). A right wrist positive contribution started at the onset of the flick phase (81.3 (0.8) %; Figure 6), coinciding with the start of wrist flexion and with the peak torso positive contribution (Figure 2). Subsequently, the right wrist positive contribution reached its peak value at ball release (100.3 (2.3) %). The left wrist positive contribution started at 87.6 (2.7) %, significantly later than the onset of the flick and right wrist positive contribution ($p < 0.001$). The peak positive contribution of the left wrist occurred at 105.2 (2.9) %, which was significantly after right wrist peak positive contribution ($p < 0.001$) and ball release ($p < 0.01$). The main contributors to stick velocity, at ball release, were trunk motions (lateral and axial rotation), right wrist flexion and left wrist extension (Figures 6 and 7), which contradicts our second hypothesis that all joints contribute substantially. The left elbow contribution at ball release was only 3.6 m/s with a relatively large standard deviation of ± 4.8 m/s. Furthermore, shoulder motions and right elbow motions did not contribute positively to stick endpoint speed at ball release.

4. Discussion and implications

This study describes the kinematic pattern that hockey players use when performing the drag flick. As hypothesised, this pattern corresponded by and large to a proximo-distal

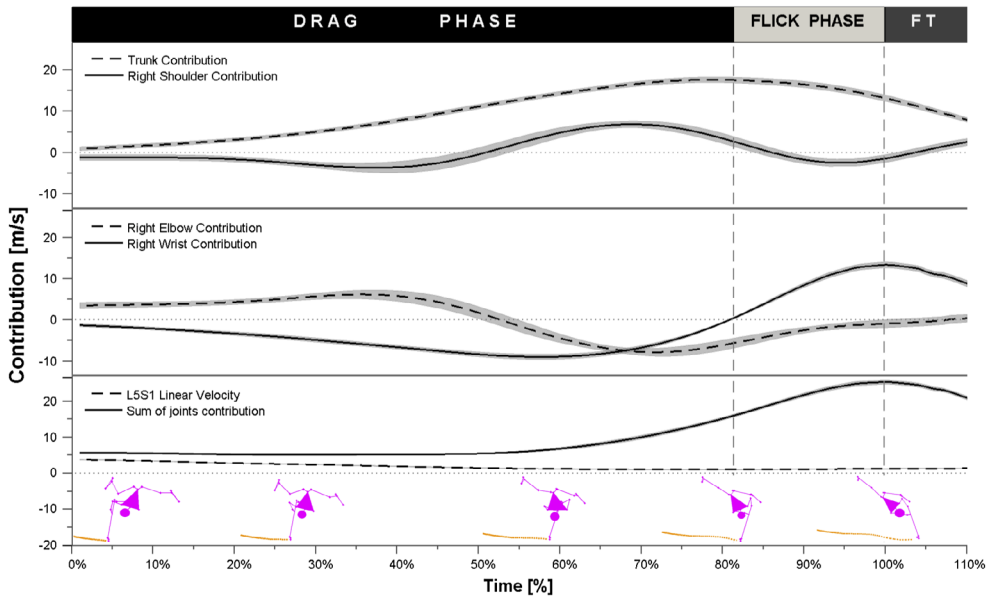


Figure 6. Trunk and right upper limb mean joints contribution to stick endpoint speed in black solid and dashed line (refer to the subfigure legend), normalised over time and averaged over participants' best trial, and the standard error in grey shading. Refer to caption of Figure 2.

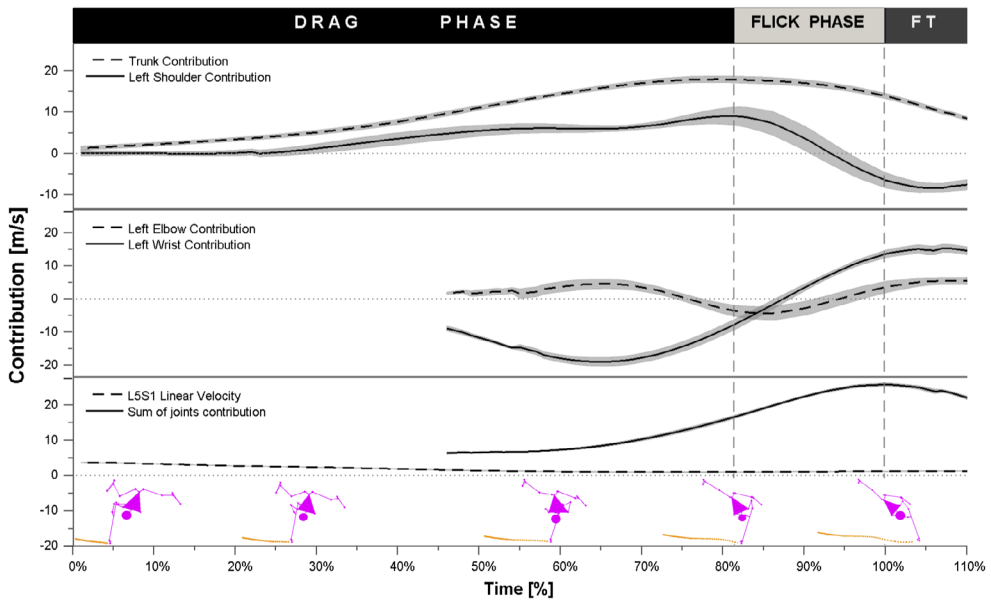


Figure 7. Trunk and left upper limb mean joints contribution to stick endpoint speed in black solid and dashed line (refer to the subfigure legend), normalised over time and averaged over participants' best trial, and the standard error in grey shading. Refer to caption of Figure 2.

sequence, predicted by the kinetic link principle, rather than reaching peaks at the same time in each joint, as predicted by the principle of optimal coordination of partial momenta.

However, due to the closed chain formed by the trunk, arms and stick, the drag flick requires some rotations of the distal segments to take place relatively early. For example, during the drag phase, peaks in right elbow supination and pronation velocity corresponded with longitudinal stick rotations made to drag the ball along with the head of the stick. Moreover, hockey players grab the stick with the hands at different levels, with the right hand placed below the left one, providing a substantial moment arm between both hands. During the lag (in the drag phase), left shoulder external rotation occurs to allow right wrist extension while keeping the ball moving in straight line. During the flick, left shoulder internal rotation occurs to allow the flicking motions of the right hand (right wrist flexion), while again keeping a straight ball trajectory. It is also assumed that left wrist radial deviation (90.4 (11.1)%) was necessary in association with left shoulder internal rotation (90.4 (6.8)%) given the constraint of the closed chain.

Right wrist flexion reached its peak velocity non-significantly before right elbow extension, which is in agreement with other ballistic but open chain movements, such as baseball pitching and handball throwing (Hong, Cheung, & Roberts, 2001; van den Tillaar & Ettema, 2004, 2009). This might be due to the presence of biarticular muscles, in this case the wrist flexors. Ettema, Styles, and Kippers (1998) showed that wrist flexor muscles have a substantial moment arm at the elbow. This biarticular function implicates that a flexion moment, caused by right wrist flexor muscles, can cause a flexion moment around the right elbow. Therefore, it can delay peak right elbow extension, which may explain why peak right elbow extension occurred slightly after peak right wrist flexion.

With the exception of the left wrist deviation, Figure 5 shows a proximo-distal sequence in both upper limbs, but differences between adjacent onset values were not always statistically significant due to the relatively large standard deviation of timing of onset of shoulder and elbow rotations. One possible limitation of this study is that we analysed rotation about multiple axes for each joint. Reporting one overall resultant angular velocity per joint might seem more useful for analysing the kinetic link principle, because it would avoid interpretation problems caused by having different onset and peak rotation timings about the individual axes within a joint. However, this approach would prevent us from quantifying positive contributions to the speed of the stick head. Figures 6 and 7 show that shoulders and elbows rotations, in contrast to our second hypothesis, did not contribute substantially to stick endpoint speed around ball release. This becomes logical when considering the directions of the rotations with angular velocities higher than 300 deg/s in these joints (Figures 2 and 3). The inconsistency in the onset of shoulders and elbows rotations may thus illustrate that these rotations are not essential for increasing ball speed. However, while these joints did not directly contribute positively to ball speed, their role was still pertinent in promoting the effect of motion of the trunk on ball speed. Specifically, they limited the effect of the decrease in trunk angular velocity on the trunk contribution by enlarging its moment arm to stick endpoint.

To explain why athletes adopt the movement pattern described, we highlighted some important time instants by inserting stick figures of the 3D model (top-view) in Figures 2, 3, 6 and 7. The drag flick demands coordinated movement of multiple joints to push the ball in a roughly straight line from its initial position towards the target. Looking at the stick figures clarifies how the moment arm of stick endpoint relative to the L5/S1 joint evolves in time and how the stick endpoint follows roughly a straight line. Shoulders and elbows extend and flex, respectively, early in the drag phase. Subsequently, they start to

flex and extend, respectively, at the end of the drag phase. The latter increases the moment arm of the stick endpoint relative to the L5S1 joint, with the longest moment arm around ball release. Moreover, these motions insure a straight ball trajectory when the torso would tend to curve it during flick phase.

One could still argue based on Figure 6 that if right wrist positive contribution to ball speed would start earlier, it could reach its peak at about the same time as peak trunk contribution (i.e. principle of optimal coordination of partial momenta). Consequently, ball release would occur earlier as well, but with a higher stick velocity, considering that trunk contribution would have been still at, roughly, its peak magnitude. This may be unattainable because at the start of the flick phase, the right wrist started to contribute positively to stick endpoint speed (Figure 6), caused by right wrist flexion angular velocity (Figure 2). Simultaneously, the trunk contribution started to decrease due to deceleration of trunk axial and lateral rotations. The transfer of angular momentum from proximal to distal segments, as the distal segments push off relative to the proximal segments when the joints start to rotate, and as the moment arm of the stick increases relative to the L5S1 joint, may be the reasons behind this decrease in trunk angular velocity (Dunn & Putnam, 1988). In addition, the nervous system may protect the joints by decelerating movements before reaching the anatomical limits (Kim, Hinrichs, & Dounskaia, 2009). However, it is uncertain which of these mechanisms (or maybe both) play a role in the drag flick. Future research could analyse the angular momentum and energy flow during the drag flick, along with measurement of muscle activity, to elucidate whether this transfer is due to a mechanical response of the trunk segment to activation of right shoulder muscles that accelerate the arm, or that it is achieved by contraction of antagonistic lower trunk muscles to protect lower trunk joints from reaching their anatomical limits (Corcos, Gottlieb, & Agarwal, 1989; Kim et al., 2009).

Given the strong non-sagittal plane trunk contribution to endpoint speed, strength and conditioning coaches should probably emphasise training drag flickers' trunk muscles, especially those contributing to dynamic trunk axial and lateral rotation motions, such as the abdominal obliques. Furthermore, right wrist flexion is a main contributor to endpoint speed and might thus be included in dynamic strength training. The shoulder and elbow motions mainly facilitate a long moment arm and a straight ball trajectory, so that coordination may be more important than power generation. These recommendations are, however, somewhat premature, given that joint contributions analysed in this study are kinematic contributions and do not directly pinpoint joint moments or muscle groups responsible for generating these movements. Future research needs to incorporate joint moments and measurement of muscle activation, to confirm the implications of our outcomes.

In addition, shoulder rotations calculated by the 3D model, in this study, are a limited representation of arm motion given the fact that we did not differentiate glenohumeral from shoulder girdle motion. The 3D model gives shoulder rotations as the motion of the arm with respect to the trunk, which neglects shoulder joint centre translation and therefore affects the length of moment arm from shoulder to stick head.

5. Conclusion

In conclusion, we present a detailed report of the kinematics of the drag flick performed by elite hockey players. They used a movement pattern, close to a proximal-to-distal sequence, in which trunk axial and lateral rotations, right wrist flexion and left wrist extension were

the main contributors to stick endpoint speed. Shoulder and elbow motions mainly insured a straight ball trajectory and elongated the trunk moment arm to stick endpoint.

Acknowledgements

The authors acknowledge the assistance of Floris Morang during data collection. The authors also thank the Hockey Club of Bloemendaal for providing their time to support this research.

Disclosure statement

No potential conflict of interest was reported by the authors.

References

- Berne, N., & Cappozzo, A. (Ed.). (1990). *Biomechanics of human movement: Applications in rehabilitation, sports and ergonomics* (pp. 89–97). Worthington, OH: Bertec Corp.
- Bobbert, M. F., Gerritsen, K. G. M., Litjens, M. C. A., & Van Soest, A. J. (1996). Why is countermovement jump height greater than squat jump height? *Medicine & Science in Sports & Exercise*, 28, 1402–1412.
- Cappozzo, A., Catani, F., Della Croce, U., & Leardini, A. (1995). Position and orientation in space of bones during movement: Anatomical frame definition and determination. *Clinical Biomechanics*, 10, 171–178.
- Corcos, D. M., Gottlieb, G. L., & Agarwal, G. C. (1989). Organising principles for single-joint movements. II. A speed sensitive strategy. *Journal of Neurophysiology*, 62, 358–368.
- De Leva, P. (1996). Joint centre longitudinal positions computed from a selected subset of Chandler's data. *Journal of Biomechanics*, 28, 1231–1233.
- Dunn, E. G., & Putnam, C. A. (1988). The influence of lower leg motion on thigh deceleration in kicking. In G. Groot, A. P. de Hollander, P. A. Huijing, & G. J. van Ingen Schenau (Eds.), *Biomechanics XI-B* (pp. 789–790). Amsterdam: Free University Press.
- Elliott, C. B., Marshall, N. R., & Noffal, J. G. (1995). Contributions of upper limb segment rotations during the power serve in tennis. *Journal of Applied Biomechanics*, 11, 433–442.
- Ettema, G. J. C., Styles, G., & Kippers, V. (1998). The moment arms of 23 muscle segments of the upper limb with varying elbow and forearm positions: Implications for motor control. *Human Movement Science*, 17, 201–220.
- Faber, G. S., Chang, C., Kingma, I., & Dennerlein, J. (2013). Lifting style and participant's sex do not affect optimal inertial sensor location for ambulatory assessment of trunk inclination. *Journal of Biomechanics*, 46, 1027–1030.
- Faber, G. S., Kingma, I., & van Dieën, J. H. (2011). Effect of initial horizontal object position on peak L5/S1 moments in manual lifting is dependent on task type and familiarity with alternative lifting strategies. *Ergonomics*, 54, 72–81.
- Hochmuth, G. (1974). *Biomechanik Sportlicher Bewegungen* [Biomechanics of sports motions] (p. 152). Berlin-Ost: Sportverlag.
- Hong, D., Cheung, K. T., & Roberts, M. E. (2001). A three-dimensional, six-segment chain analysis of forceful overarm throwing. *Journal of Electromyography and Kinesiology*, 11, 95–112.
- Jennings, M. J., Blanchonette, I., Lucas, S. R., Morgan, S. W., Helmer, R. J. N., & Yang, C. (2010). Instrumentation of a field hockey stick to detect stick and ball interaction during a drag flick. *Procedia Engineering*, 2, 2979–2984.
- Kellis, E., & Katis, A. (2007). Biomechanical characteristics and determinants of instep soccer kick. *Journal of Sports Science & Medicine*, 6, 154–165.
- Kim, Y.-K., Hinrichs, R. N., & Dounskaia, N. (2009). Multicomponent control strategy underlying production of maximal hand velocity during horizontal arm swing. *Journal of Neurophysiology*, 102, 2889–2899.

- Kingma, I., de Looze, P. M., Toussaint, M. H., Klijnsma, G. H., & Bruijnen, B. M. T. (1996). Validation of a full body 3-D dynamic linked segment model. *Human Movement Science*, 15, 833–860.
- Liu, H., Leigh, S., & Yu, B. (2010). Sequences of upper and lower extremity motions in javelin throwing. *Journal of Sports Sciences*, 28, 1459–1467.
- López de Subijana, C., Juarez, D., Mallo, J., & Navarro, E. (2010). Biomechanical analysis of the penalty-corner drag flick of elite male and female hockey players. *Sports Biomechanics*, 9, 72–78.
- Marshall, R. N., & Elliott, B. C. (2000). Long-axis rotation: The missing link in proximal-to-distal segmental sequencing. *Journal of Sports Sciences*, 18, 247–254.
- McLaughlin, P. (1997). *Three dimensional biomechanical analysis of the hockey drag flick: Full report*. Australia: National Sports Research Centre. (ISBN 0 642 26313 2).
- Piñero, R., Sampedre, J., & Refoye, I. (2007). Differences between international men's and women's teams in the strategic action of the penalty corner in field hockey. *International Journal of Performance Analysis in Sport*, 7, 67–83.
- Putnam, A. C. (1993). Sequential motions of body segments in striking and throwing skills: Descriptions and explanations. *Journal of Biomechanics*, 26, 125–135.
- Reeser, C. J., Fleisig, S. G., Bolt, B., & Ruan, M. (2010). Upper limb biomechanics during the volleyball serve and spike. *Sports Health: A Multidisciplinary Approach*, 2, 368–374.
- van den Tillaar, R., & Ettema, G. (2004). A force-velocity relationship and coordination patterns in overarm throwing. *Journal of Sports Science and Medicine*, 3, 211–219.
- van den Tillaar, R., & Ettema, G. (2009). Is there a proximal-to-distal sequence in overarm throwing in team handball? *Journal of Sports Sciences*, 27, 949–955.
- Wagner, H., Pfustershmed, J., Von Duvillard, P. S., & Müller, E. (2011). Skill-dependent proximal-to-distal sequence in team-handball throwing. *Journal of Sports Sciences*, 30, 21–29.
- Yusoff, S., Hasan, N., & Wilson, B. (2008). Three- dimensional biomechanical analysis of the hockey drag flick performed in competition. *ISN Bulletin, National Sport Institute of Malaysia*, 1, 35–43.

Appendix 1.

Table indicating body segments and related bony landmarks used in the present study. Local axes systems were reconstructed based on the anatomical landmarks. In addition, cluster markers used to track motions of the respective segments are indicated. Note that leg segments are not used for the present analyses.

Body segments (related marker clusters)	Corresponding anatomical landmarks
Foot (shank)	2nd toe tip; Calcaneus; lateral and medial malleolus
Shank (shank)	Lateral and medial malleolus; lateral and medial femur epicondyles
Thigh (shank and pelvis)	Lateral and medial femur epicondyles; greater trochanter
Pelvis (pelvis)	Right and left antero-superior iliac spines; midpoint between the postero-superior iliac spines; navel
Abdomen (thorax)	Navel; 12th thoracic (T12); xiphoid process
Thorax (thorax)	Xiphoid process; 6th thoracic (T6); suprasternal; 7th cervical (C7)
Head (thorax)	7th cervical (C7); right and left tragon; head vertex
Upper arm (upper arm)	Acromion process; lateral and medial humeral epicondyles
Forearm (forearm)	Lateral and medial humeral epicondyles; radial and ulnar styloids